

# Regulation of *Arabidopsis* shoot apical meristem and lateral organ formation by microRNA *miR166g* and its *AtHD-ZIP* target genes

Leor Williams<sup>1</sup>, Stephen P. Grigg<sup>1,\*</sup>, Mingtang Xie<sup>2</sup>, Sioux Christensen<sup>2</sup> and Jennifer C. Fletcher<sup>1,†</sup>

<sup>1</sup>Plant Gene Expression Center, USDA/UC Berkeley, 800 Buchanan Street, Albany, CA 94710, USA

<sup>2</sup>Dept of Molecular, Cellular and Developmental Biology, UCLA, Los Angeles, CA 90095, USA

\*Present address: Department of Plant Sciences, Oxford University, Oxford OX1 3RB, UK

†Author for correspondence (e-mail: fletcher@nature.berkeley.edu)

Accepted 13 June 2005

Development 132, 3657-3668

Published by The Company of Biologists 2005

doi:10.1242/dev.01942

## Summary

Plant development is characterized by precise control of gene regulation, leading to the correct spatial and temporal tissue patterning. We have characterized the *Arabidopsis jabba-1D* (*jba-1D*) mutant, which displays multiple enlarged shoot meristems, radialized leaves, reduced gynoecia and vascular defects. The *jba-1D* meristem phenotypes require *WUSCHEL* (*WUS*) activity, and correlate with a dramatic increase in *WUS* expression levels. We demonstrate that the *jba-1D* phenotypes are caused by over-expression of *miR166g*, and require the activity of the RNase III helicase *DCL1*. *miR166g* over-expression in *jba-1D* plants affects the transcripts of several class III homeodomain-leucine zipper (*AtHD-ZIP*) family

target genes. The expression of *PHABULOSA* (*PHB*), *PHAVOLUTA* (*PHV*) and *CORONA* (*CNA*) is significantly reduced in a *jba-1D* background, while *REVOLUTA* (*REV*) expression is elevated and *ATHB8* is unchanged. In addition, we show that *miR166* has a dynamic expression pattern in wild-type and *jba-1D* embryos. Our analysis demonstrates an indirect role for miRNAs in controlling meristem formation via regulation of *WUS* expression, and reveals complex regulation of the class III *AtHD-ZIP* gene family.

Key words: microRNA, *Arabidopsis thaliana*, shoot apical meristem, polarity, HD-ZIP

## Introduction

Eukaryotic development requires the precise spatial and temporal expression of regulatory genes that pattern tissues and control cell fate. It is becoming increasingly clear that small RNA molecules are important participants in these processes, providing sequence specificity for targeted regulation of key developmental factors at the post-transcriptional level. microRNAs (miRNAs) are 21-24 nucleotide single-stranded RNA molecules found in both plants and animals that can down-regulate gene expression by pairing to the messages of protein-coding genes (Bartel, 2004). They are produced from larger precursor transcripts of ~70-300 nucleotides in length that contain a characteristic hairpin secondary structure. In plants, mature miRNA sequences are processed from the double-stranded hairpin region of the precursor molecules by *DICER-LIKE1* (Schauer et al., 2002), a ribonuclease III helicase protein that acts as a dsRNA-specific endonuclease (Park et al., 2002; Reinhart et al., 2002). The novel protein *HEN1* and the nuclear dsRNA-binding protein *HYL1* are also required for plant miRNA accumulation (Han et al., 2004; Park et al., 2002; Vazquez et al., 2004).

miRNAs appear to regulate gene expression by binding to complementary sequences in the mRNA transcripts produced by their target genes (Bartel, 2004). While animal miRNAs tend to have several mismatches with their target mRNA sequences, plant miRNAs are characterized by their near-perfect complementarity with their targets (Rhoades et al.,

2002). Interaction of the miRNA with its target mRNA sequence is recognized by an RNA-induced silencing complex (RISC), leading either to specific cleavage of the mRNA via RISC endonuclease activity, or to translational repression (reviewed by Bartel, 2004). The RISC has been purified from fly and human cells (Hammond et al., 2000; Martinez et al., 2002), and in both cases contains a member of the ARGONAUTE (AGO) family of PPD proteins (Cerutti et al., 2000). *Arabidopsis* plants with reduced *AGO1* gene activity accumulate mRNAs that are normally targeted for miRNA-mediated cleavage, confirming a role for AGO1 in the miRNA regulatory pathway (Vaucheret et al., 2004).

Mutants that lack *DCL1* activity are embryo lethal (Schauer et al., 2002), revealing that miRNA metabolism is essential for normal plant development. Similarly, plants carrying weaker *dcl1* alleles survive embryogenesis but display a wide spectrum of developmental defects (Schauer et al., 2002), while *hen1* and *hyl1* null mutants show reduced miRNA levels and morphological phenotypes that overlap with those of weak *dcl1* alleles (Han et al., 2004; Park et al., 2002; Vazquez et al., 2004). *ago1* null mutants are viable but have pleiotropic developmental phenotypes (Bohmert et al., 1998), while *ago1* hypomorphic mutants exhibit morphological defects similar to those of *dcl1*, *hen1* and *hyl1* mutants (Vaucheret et al., 2004).

Consistent with the demonstration that activity of the miRNA pathway is important for plant development, it has been observed that a large fraction of the predicted target transcripts of plant miRNAs encode members of transcription

factor families (Rhoades et al., 2002). Many of these transcription factors have defined or predicted roles in developmental patterning, phase transition and/or cell fate control (Bartel, 2004). A direct role for miRNAs in regulating different aspects of *Arabidopsis* development has been experimentally demonstrated in a number of cases (Achard et al., 2004; Aukerman and Sakai, 2003; Baker et al., 2005; Chen, 2004; Emery et al., 2003; Mallory et al., 2004; Palatnik et al., 2003; Zhong and Ye, 2004).

Among the *Arabidopsis* developmental regulators targeted by miRNAs are five members of the class III homeodomain-leucine zipper (HD-ZIP) family of transcription factors (Sessa et al., 1998), *REVOLUTA* (*REV*), *PHABULOSA* (*PHB*), *PHAVOLUTA* (*PHV*), *CORONA* (*CNA*) and *ATHB8*. Loss-of-function *phb*, *phv*, *cna* and *athb8* mutants are aphenotypic (Baima et al., 2001; Prigge et al., 2005), but *rev* mutants form defective lateral and floral meristems and develop aberrant stem vasculature (Otsuga et al., 2001; Talbert et al., 1995). *rev phb phv* triple mutants fail to establish a shoot apical meristem and produce abaxialized cotyledons, indicating that these three genes play overlapping roles in regulating SAM formation, leaf polarity and radial patterning (Emery et al., 2003; Prigge et al., 2005). *PHB*, *PHV* and *CNA* have overlapping functions in regulating meristem size, lateral organ polarity and vascular development that are distinct from *REV* (McConnell and Barton, 1998; McConnell et al., 2001; Prigge et al., 2005). *ATHB8* has been proposed to play a role in vascular development (Baima et al., 1995; Baima et al., 2001), and acts redundantly with *CNA* to promote post-embryonic meristem activity (Prigge et al., 2005).

The five class III HD-ZIP gene transcripts are targeted by miRNAs from the *miR165/166* group. Two *MIR165* genes and seven *MIR166* genes are encoded in the *Arabidopsis* genome, and the mature *miR165* and *miR166* sequences differ from one another by a single nucleotide (Reinhart et al., 2002). In wheat germ extracts, *miR165/166* guides the RISC to efficiently cleave wild-type *PHV* mRNA (Tang et al., 2003) and *CNA/ATHB15* mRNA (Kim et al., 2005). Increased expression of *miR166a* in an activation-tagged line causes a reduction in *PHB*, *PHV* and *CNA* transcript levels, leading to an expansion of xylem tissue and the interfascicular region, indicative of accelerated vascular cell differentiation (Kim et al., 2005). Stem fasciation and SAM enlargement are also reported in the *miR166a* over-expression line. Conversely, *phv*, *phb* and *rev* gain-of-function alleles that alter the *miR165/166* complementary site are resistant to mRNA cleavage mediated by *miRNA165/166* (Emery et al., 2003; Tang et al., 2003; Mallory et al., 2004; Zhong and Ye, 2004), and they confer specific patterning phenotypes as a result of ectopic expression of their target gene products (Emery et al., 2003; McConnell and Barton, 1998; McConnell et al., 2001; Zhong and Ye, 2004).

Using an activation tagging approach, we demonstrate that *miR166g* causes de novo SAM formation and disrupts the morphogenesis of leaves, vascular bundles and gynoecia when over-expressed in *Arabidopsis*. We show that *jba-1D* meristem cells express much higher than normal levels of *WUS* mRNA, and that *WUS* activity is required to obtain the *jba-1D* meristem phenotype. We find that *miR166* is expressed in a dynamic pattern in developing wild-type and *jba-1D* embryos, being largely complementary to its HD-ZIP target transcripts in early

stages but coincident with them in later stages. Over-expression of *miR166g* causes reduced accumulation of *PHB*, *PHV* and *CNA* transcripts in *jba-1D* seedlings and inflorescence apices. Increased accumulation of *REV* transcripts is also detected, but is not sufficient to account for the meristem defects. We propose that down-regulation of *PHB*, *PHV* and *CNA* mRNAs in *jba-1D* plants leads to up-regulation of *WUS* transcription in the SAM organizing center, which results in splitting and fasciation of the primary shoot apex.

## Materials and methods

### Plant growth and genetic analysis

Plants were grown in a 1:1:1 mixture of perlite:vermiculite:top soil under continuous cool-white fluorescent lights (120  $\mu\text{mol/m}^2/\text{second}$ ) at 22°C. Double mutants with *dcl1-9*, *wus-1* and *rev-6* were generated by crossing *jba-1D/+* plants to *dcl1-9/+* or *wus-1/+* or *rev-6* plants, and identified by PCR genotyping the F<sub>1</sub> and F<sub>2</sub> progeny. Control crosses to Col were performed with both *dcl1-9* and *wus-1*, which originated from the *Ler* ecotype. The plasmid for recapitulating the *jba* phenotype was generated by amplifying from *jba-1D* genomic DNA a 1254 base pair fragment spanning from the 35S enhancers in the T-DNA right border to 129 base pairs downstream of the *MIR166* locus. The amplified fragment was cloned into pBIN binary vector. Plant transformation was performed using the floral dip method (Clough and Bent, 1998).

### Microscopy

Scanning electron microscopy was performed as described previously (Bowman et al., 1989) using a Hitachi 4700 scanning electron microscope with digital imaging capability. Confocal scanning electron microscopy analysis was performed as described (Running et al., 1995) using a LSM Zeiss 510 confocal microscope.

### Histology

Tissues were fixed, embedded in Technovit 7100 resin, sectioned at 5  $\mu\text{m}$  thick and stained in Toluidine Blue solution as described previously (Smith and Hake, 2003).

### GUS staining

The GUS staining reaction and subsequent tissue embedding and sectioning were performed as described previously (Sieburth and Meyerowitz, 1997) using 2 mM 5-bromo-4-chloro-3-indolyl- $\beta$ -D-glucuronide (X-GLUC; Bioworld, Dublin, OH, USA).

### In situ hybridization

Tissue fixation and in situ hybridization were performed as described previously (Jackson, 1992). Probes for in situ hybridization were transcribed using the digoxigenin labeling mix (Roche). For the *REV* probe, the full-length cDNA was used as a template. For the *CNA* and *PHB* probes, the nucleotide regions 1230-2511 and 1285-2554, respectively, relative to the ATG, were used as templates. For the *miR166* probe, four concatamers of sense or antisense sequences were synthesized as oligonucleotides and cloned into pBS-SK. Hybridization with the *miR166* probe was carried out at 42°C overnight. After hybridization, the slides were washed four times at 40°C for 10 minutes each.

### Real-time and RT-PCR

Aerial parts of 28-day Col and *jba-1D* homozygous plants were used for real-time PCR analysis. cDNA synthesis was carried out in a 20  $\mu\text{l}$  reaction using 1  $\mu\text{g}$  DNase I-treated total RNA by the reverse transcription system (Promega). The cDNA reaction mixture was diluted 1:10 using DNase-, RNase-free Milli-Q water and 1  $\mu\text{l}$  was taken for real-time amplifications. Amplifications were carried out in



duplicate on 96-well plates in a 25  $\mu$ l reaction volume containing 12.5  $\mu$ l 2 $\times$  SYBR Green Supermix (Bio-Rad), 0.25  $\mu$ M each of forward and reverse primers and 1  $\mu$ l of the 1:10-diluted cDNA. All reactions were performed independently twice on iCycler (Bio-Rad) and once on DNA Engine Opticon (MJ Research, Hercules, CA, USA) to ensure reproducibility. For all samples the cDNA levels were normalized using a ubiquitin control. For RT-PCR analysis, total RNA was isolated from 9-day-old seedlings and inflorescences using the RNeasy plant kit (Qiagen). The samples were treated with RQ1 RNase-free DNase (Promega) for 30 minutes at 37°C and then purified with phenol/chloroform. First strand cDNA synthesis was performed on 5 mg of total RNA using Superscript III RNase H<sup>-</sup> reverse transcriptase (RT) (Gibco-BRL, Life Technologies) and an oligo(dT) primer according to the manufacturer's instructions. Of the 20  $\mu$ l of the RT reaction 1  $\mu$ l was used for each PCR reaction. For *CNA*, *PHB*, *PHV* and *ATHB8*, 30 cycles of PCR were performed; for *REV*, 25 cycles of PCR were performed. The annealing temperature was 62°C for all genes. The set of primers used for all five genes flank the *miR166* recognition sequence: (*REV* S-ggattgctctcaatcgagagg, AS-ctcacaactgagaagctgaagc; *PHB* S-ggactccttctatagcagaggagg, AS-aaagtttgaagaaggtgccccag; *PHV* S-tgcccggaggagaccttggcg, AS-gatagtagaccatttccagtg; *ATHB8* S-cttgaccctcaacatcagcctc, AS-gcaagcagcagcagcg-attccc; *CNA* S-caattggcatctcaaatcctcag AS-gggccaagtgtagttgggtcatag). The primers used to amplify the control *EF1 $\alpha$*  gene are S-caggctgattgtgctgtcttcat and AS-cttgtagacatcctgaagtgtggaaga.

#### Small RNA isolation and blot analysis

RNA isolation and RNA filter hybridization were performed as described previously (Chen, 2004). Blots were hybridized using *miR166* antisense end-labeled oligonucleotides. As a ladder, a mixture of 0.1  $\mu$ M *miR166* sense oligonucleotides and 0.1  $\mu$ M *miR166* sense plus 13 nucleotides was loaded on a gel. Primer sequences are available on request.

## Results

### A dominant mutant affecting *Arabidopsis* morphogenesis

The *jabba-1D* (*jba-1D*) mutant was isolated in a population of Columbia (Col) plants carrying the pSKI015 activation tagging T-DNA vector (Weigel et al., 2000). Upon insertion into genomic DNA, the tandem repeat of four CaMV35S enhancers adjacent to the T-DNA right border can activate or enhance the expression of nearby genes. Typically the 35S enhancer elements up-regulate the affected gene in its normal expression domain, rather than inducing ectopic expression of the gene in a novel domain (Weigel et al., 2000).

Analysis of hemizygous and homozygous *jba-1D* plants revealed three distinct morphological phenotypes (Fig. 1). The most dramatic *jba-1D/+* phenotype was extreme fasciation of the flowering shoot apical meristem (inflorescence meristem), which caused the stem to grow as a wide strap-like structure rather than as a point (Fig. 1B). The second phenotype was a reduced or filamentous gynoeceum, which rendered the hemizygous plants less fertile than their wild-type siblings (Fig. 1G). The third phenotype was epinastic leaf morphology (Fig. 1K). Homozygous *jba-1D* plants had more dramatic leaf

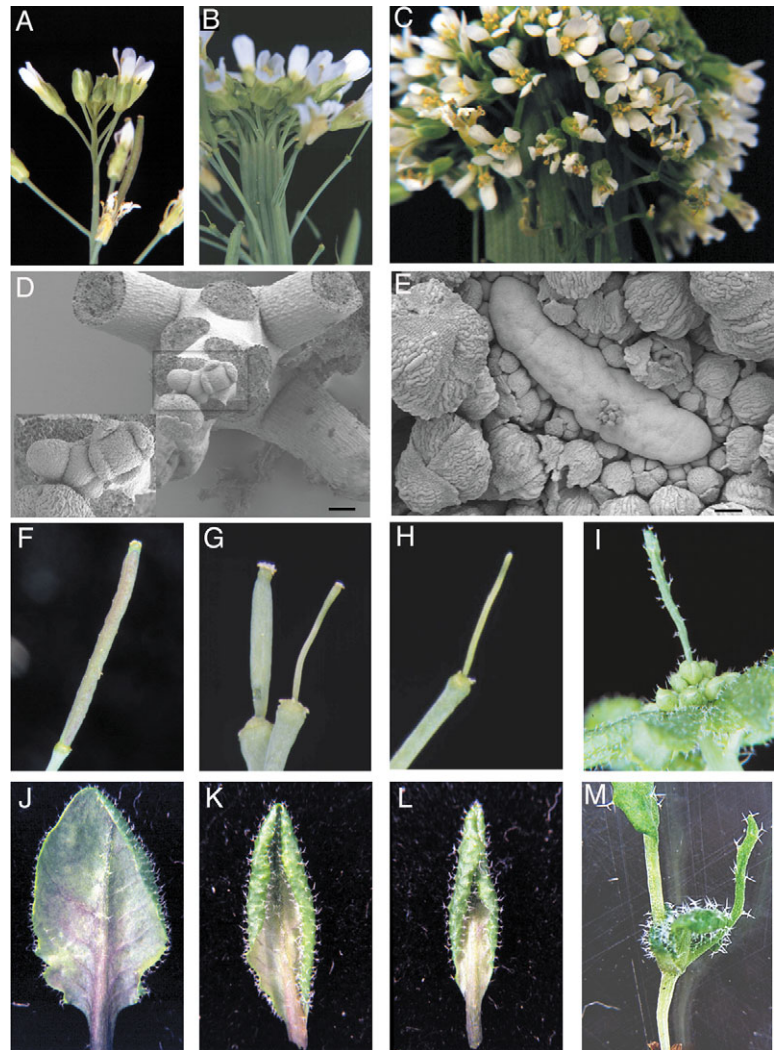


**Fig. 1.** *jba-1D* morphological phenotypes are dose dependent. (A) Wild-type Columbia (Col) inflorescence stem. (B) Fasciated *jba-1D/+* stem. (C) Severely fasciated *jba-1D* stem. (D) SEM of a wild-type inflorescence meristem. Inset: an enlargement of the shoot tip (the boxed region). (E) SEM of a fasciated *jba-1D* inflorescence meristem. (F) Wild-type silique consisting of two fused carpels. (G) Reduced and filamentous *jba-1D/+* siliques. (H) Filamentous *jba-1D* silique. (I) Radialized leaf projecting outward from the center of a *jba-1D* inflorescence meristem. (J) Wild-type rosette leaf, viewed from the abaxial side. (K) Slightly downward curled *jba-1D/+* rosette leaf. (L) Severely downward curled *jba-1D* rosette leaf. (M) Completely radialized rosette leaf from a *jba-1D* seedling. Scale bars: 60  $\mu$ m (D,E).

phenotypes, producing severely downward curling and radialized leaves (Fig. 1L,M). *jba-1D* plants also displayed more extreme inflorescence meristem and flower phenotypes than *jba-1D/+* plants, and were completely sterile (Fig. 1C,H). Thus the developmental phenotypes appeared to be dose-dependent – a single copy of this dominant mutation was sufficient to confer the phenotypes, but two copies made the phenotypes more severe. Pollen dehiscence was also reduced in *jba* hemizygous and homozygous plants, but all other aspects of development appeared to be unaffected by the mutation.

Examination of *jba-1D* plants revealed that at the transition to flowering, when the *jba* SAM phenotype becomes visible to



the naked eye, both *jba-1D/+* and *jba-1D* plants had extremely enlarged primary inflorescence meristems (Fig. 2). In *jba-1D/+* plants, the inflorescence meristems were both taller and wider than wild-type meristems, but the structural organization of the meristems was intact (Fig. 2A,B). In *jba-1D* plants, the primary reproductive shoot apex consisted of multiple, independently organized SAMs (Fig. 2C). Large numbers of floral meristems were initiated from each of the *jba-1D* inflorescence meristems, which continued to accumulate excess cells such that the shoot apices were ultimately visible to the naked eye (Fig. 1E). We interpret this phenotype as a hyper-activation of SAM activity that becomes progressively more severe during reproductive development. In contrast, the size of *jba-1D* floral meristems was only slightly increased relative to wild-type floral meristems, and floral organ number was relatively normal except for carpel number, which was reduced in *jba-*

*1D/+* flowers and essentially absent in *jba-1D* flowers (see Fig. S1 in supplementary material).

To determine when the *jba* SAMs first began to enlarge relative to wild-type SAMs, we assessed whether the vegetative meristems of *jba-1D* seedlings were distinguishable from those of wild-type seedlings. Sections through 11-day-old wild-type, *jba-1D/+* and *jba-1D* seedlings revealed that the mutants already had enlarged vegetative SAMs that were both wider and taller than wild-type SAMs (Fig. 2D-F). In fact, *jba-1D* SAMs were measurably larger than wild-type SAMs by the time the embryos reached maturity. *jba-1D* mutant embryonic meristems were  $36.6 \pm 1.1 \mu\text{m}$  wide and  $5.4 \pm 1.2 \mu\text{m}$  tall ( $n=12$ ), while Col embryonic meristems were  $28.8 \pm 1.6 \mu\text{m}$  wide and  $5.3 \pm 1.1 \mu\text{m}$  tall ( $n=9$ ). The cells in *jba-1D* embryonic SAMs were approximately the same size as cells in wild-type SAMs, indicating that the mutant SAMs consisted of more cells than

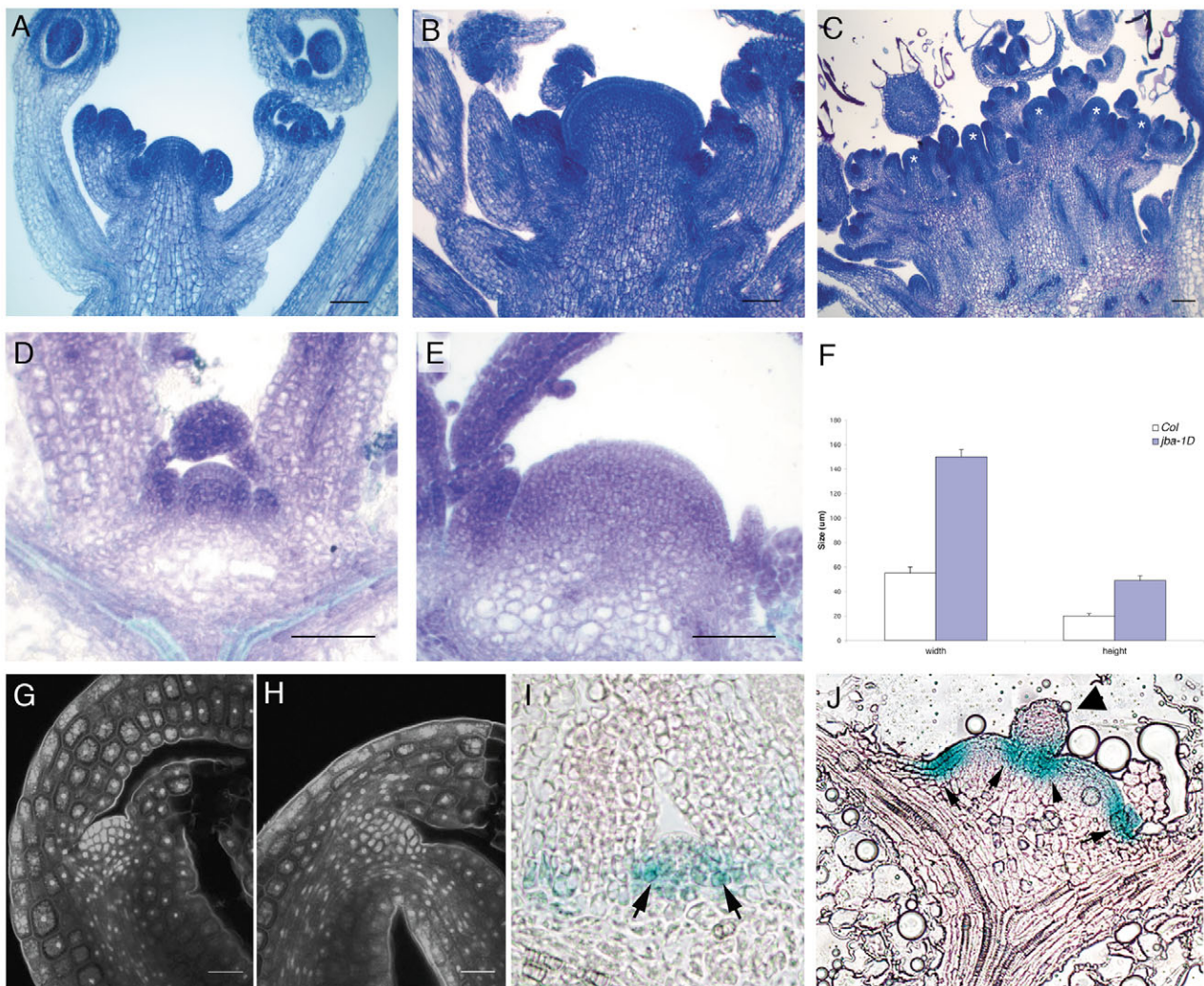


**Fig. 2.** *jba-1D* shoot apical meristem phenotypes. (A) Wild-type inflorescence meristem at the transition to flowering. (B) *jba-1D/+* inflorescence meristem that is both taller and wider than normal. (C) *jba-1D* inflorescence meristem that has split into multiple independent meristems (\*), each generating floral meristem primordia on its flanks. (D) Wild-type seedling SAM after 11 days of vegetative growth. (E) Enlarged *jba-1D* seedling SAM. (F) Mean width and height of Col ( $n=12$ ) and *jba-1D* ( $n=11$ ) SAMs from 11-day-old seedlings. (G) Confocal micrograph of a wild-type mature embryo SAM. (H) Confocal micrograph of an enlarged *jba-1D* mature embryo SAM. (I) GUS expression from a *pSTM::GUS* reporter construct in the peripheral region (arrows) of a wild-type seedling SAM. (J) *pSTM::GUS* expression in a *jba-1D* seedling delimits two well-defined meristems, while the leaf primordium developing between them is radialized (arrowhead). Scale bars: 80  $\mu\text{m}$  (A-E); 20  $\mu\text{m}$  (G-H).

those of the wild type rather than larger cells. The organization of the *jba-1D* embryonic and vegetative meristems was not disturbed.

We confirmed the *jba-1D* SAM splitting phenomenon by using *pSTM::GUS* as a marker for the meristem boundary. This construct drives GUS expression at the SAM periphery, between the central region of the SAM and the developing lateral organ primordia (Fig. 2I). We found that after 11 days of vegetative growth, some *jba-1D* shoot apices consisted of two well-defined meristems rather than one single primary meristem. Each meristem was marked by *pSTM::GUS* expression at the periphery (Fig. 2J). Multiple meristems were never observed in *jba-1D* embryos, indicating that this phenomenon occurs de novo during post-embryonic development.

Cell fate in the SAM is controlled via a regulatory pathway involving the WUSCHEL (*WUS*) and CLAVATA (*CLV*) gene products (reviewed by Carles and Fletcher, 2003). The *WUS* gene is expressed in the central, interior region of the SAM, and encodes a homeodomain transcription factor that confers stem cell fate on the overlying cell population (Mayer et al., 1998; Schoof et al., 2000). *CLV3* is expressed in the stem cells, and encodes a small, secreted polypeptide that limits the size of the *WUS* expression domain (Brand et al., 2000; Fletcher et al., 1999; Rojo et al., 2002). Using promoter-GUS constructs we determined that the *WUS* expression domain (Fig. 3A-D) and the *CLV3* expression domain (Fig. 3E-F) enlarged coordinately in *jba-1D* SAMs, indicating that the fasciated meristem phenotype of *jba-1D* plants is due to the presence of many excess stem cells. In addition, we found that the distribution of *pWUS::GUS* expression was not uniform, and in some cases we observed two adjacent foci of *WUS* expression within the primary meristem (Fig. 3D). The

appearance of such foci of *WUS* expression in *jba-1D* plants can explain the observed meristem phenotype, where independent domains of *WUS* expression lead to the formation of discrete, ectopic meristems. In serial longitudinal sections through entire 11-day old *jba-1D* seedlings, no *WUS* expression was detected outside of the shoot apical meristem.

In our *pWUS::GUS* experiments, we noted that GUS expression was detected in *jba-1D* meristems after a shorter incubation time than wild-type Col meristems (compare Fig. 3B and C), suggesting that cells in *jba-1D* SAMs might express higher levels of *WUS* mRNA than those in wild-type SAMs. To test this hypothesis we performed real-time quantitative RT-PCR (qRT-PCR) on aerial parts of 28-day-old wild-type and *jba-1D* plants using primers directed against *CLV3* and *WUS*. We found that, while the relative level of *CLV3* transcription was unchanged between wild-type and *jba-1D* plants, the level of *WUS* transcription was ~12-fold higher in *jba-1D* plants compared to wild-type plants (Fig. 3G). We next determined whether *WUS* function was sufficient to produce the *jba* meristem phenotypes by generating double mutants between *jba-1D* plants and plants carrying the *wus-1* null allele. *wus-1 jba-1D* double mutant meristems were indistinguishable from *wus-1* mutant meristems (see Fig. S2 in supplementary material), indicating that *WUS* activity is absolutely required to obtain the *jba* SAM phenotypes. Taken together, our evidence indicates that the presence of elevated levels of *WUS* transcription in *jba-1D* shoot apical meristems is sufficient to account for the fasciation and de novo meristem formation phenotypes.

We further examined the *jba-1D* fasciation phenotype by analyzing the stem vascular patterning. In wild-type *Arabidopsis* plants, the vascular tissue in the stem is present as a ring of approximately five to eight separate bundles (Fig. 4A).

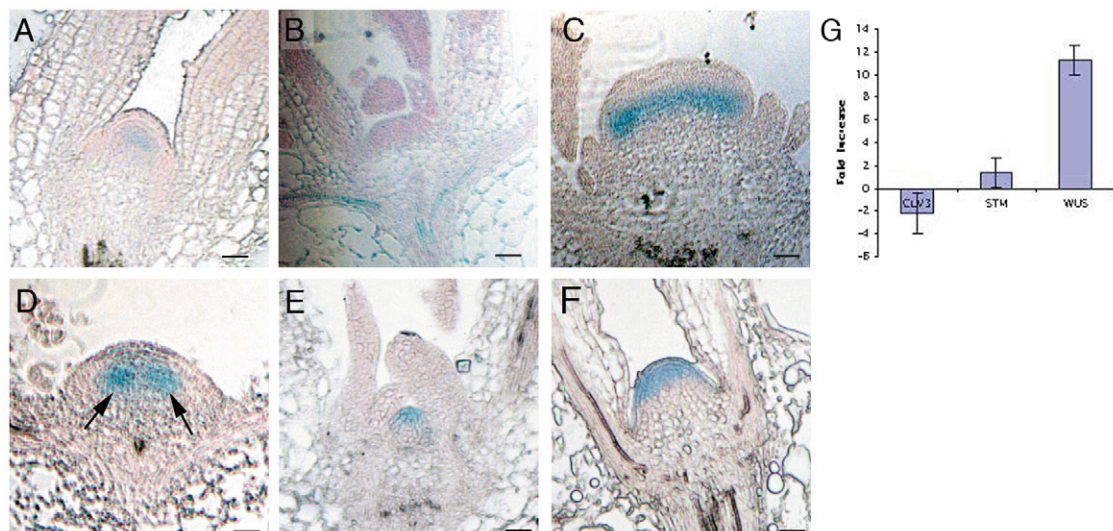


**Fig. 3.** *WUS* and *CLV3* expression in *jba-1D* shoot apical meristems. (A) GUS expression from a *pWUS::GUS* reporter construct in a wild-type seedling SAM, after 1 hour incubation in X-Gluc substrate. (B) No *pWUS::GUS* activity is detected in a wild-type seedling SAM after 20 minute incubation in X-Gluc substrate. (C) *pWUS::GUS* activity is readily detected in a *jba-1D* seedling SAM after 20 minute incubation in X-Gluc substrate. The *WUS* expression domain also expands laterally in the *jba-1D* SAM. (D) In some *jba-1D* seedlings, two independent foci of *WUS* expression are observed (arrows). (E) GUS expression from a *pCLV3::GUS* reporter construct in a wild-type seedling SAM. (F) The *CLV3* expression domain expands laterally in a *jba-1D* seedling SAM, coordinate with the expansion of the *WUS* expression domain. All seedlings are 11 days old. (G) *CLV3* and *WUS* mRNA transcription levels in Col and *jba-1D* inflorescences and floral meristems as determined by real-time qRT-PCR. Scale bars: 40  $\mu$ m.



The vascular bundles are collateral, with xylem positioned close to the center of the stem and phloem in more peripheral positions (Turner and Sieburth, 2001). Cross sections of the inflorescence stem revealed three types of alterations in the vascular patterning of *jba-1D* plants. First, *jba-1D* stems had increased numbers of discrete vascular bundles in peripheral

positions along the stem (Fig. 4C). In the most extremely fasciated *jba-1D* stems, as many as 29 individual bundles could be observed. Second, *jba-1D* mutant stems displayed defects in the organization of the vascular cell types within these bundles. The wild-type collateral pattern of xylem toward the inside and phloem toward the outside (Fig. 4B) was disrupted in *jba-1D* stems by the appearance of ectopic xylem elements close to the periphery (Fig. 4D,F). This suggests a defect in the *jba-1D* plants in the production, reception or interpretation of positional signals that pattern the vasculature. Third, *jba-1D* mutants formed extra bundles abnormally located in the center of the stem (Fig. 4C). These bundles exhibited an amphivasal arrangement, with xylem surrounding phloem (Fig. 4E), and might represent veins from the multiply splitting meristems and/or from the radial leaves that protrude from the shoot apex. These results reveal that the *jba-1D* mutation affects the number, positioning and polarity of stem vascular bundles.

The striking phenotype of radial leaf formation between two or more adjacent meristems (see Fig. 2J and Fig. S1M in the supplementary material) in *jba-1D* plants led us to analyze the morphology and vascular patterning of these leaves. Examination of the radialized leaves using light and scanning electron microscopy indicated that the leaves had adaxial features, such as trichomes and jigsaw-shaped cells, around the entire circumference (data not shown). The interior morphology of the radial rosette leaves also showed radial symmetry, with the cells resembling adaxial palisade mesophyll (Fig. 4G). However, the single vascular bundle within each radial leaf still exhibited polarity, with xylem on one side and phloem on the other side (Fig. 4H). In contrast, adaxialized radial leaves from other dominant leaf polarity mutants such as *phb-1D* exhibit radialized vascular bundles, with xylem surrounding phloem (McConnell and Barton, 1998). One interpretation of these data is that the developing *jba-1D* leaf may receive a normal adaxial polarizing signal from the SAM from which it is derived as well as weaker signals for adaxialization from adjacent meristems, leading to partial but incomplete radialization.

Since *jba-1D* plants show very similar shoot meristem and vascular phenotypes to those of the *REV* gain-of-function mutants *avb1* and *rev-10D* (Emery et al., 2003; Zhong and Ye, 2004), we tested the contribution of *REV* to the *jba-1D* phenotype by crossing *jba-1D* plants to previously described *rev-6* mutant plants (Otsuga et al., 2001). The *REV* locus and the *jba-1D* T-DNA insertion site are tightly linked on chromosome 5 with an estimated recombination frequency of 3.2% (~5 cM). From 250 F<sub>2</sub> plants that were selected on plates for the *jba-1D* T-DNA insertion, we were able to identify three *jba-1D/+ rev/rev* plants. Analysis of these plants showed that the *rev-6* mutation does not suppress the *jba-1D/+* stem fasciation phenotype (see Fig. S2 in supplementary material). This result shows that wild-type *REV* function is not essential for the stem fasciation of *jba* plants. In contrast, radial leaves are not observed in the *jba-1D/+ rev/rev* plants, indicating that *REV* does play a role in conditioning the *jba* leaf phenotypes.

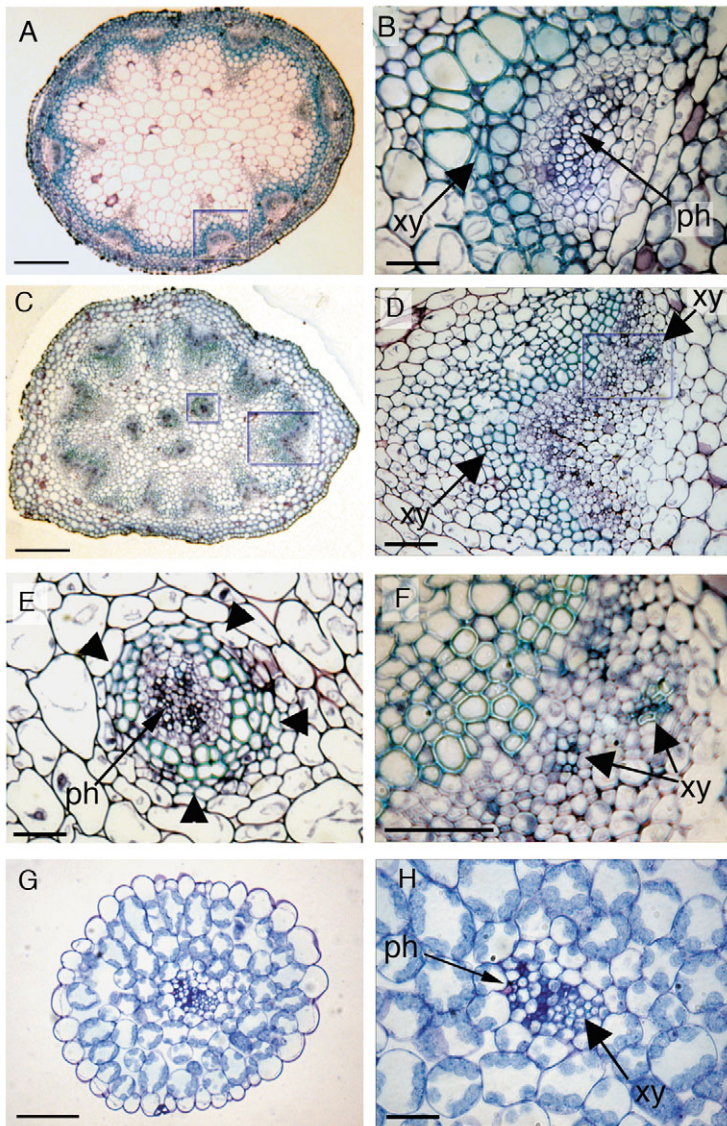


**Fig. 4.** Defective *jba-1D* inflorescence stem vasculature and lateral organ polarity. (A) Cross section through a wild-type stem. (B) Higher magnification of the boxed region in A. The vascular bundle consists of xylem (xy) located on the inner side of the bundle and phloem (ph) located on the outer side of the bundle. (C) Cross section through a *jba-1D* stem showing additional vascular bundles at the periphery and ectopic vascular bundles in the center of the stem. (D,F) Higher magnification of the boxed region in C and the boxed region in D, respectively. Xylem elements can be detected ectopically on the outer side of the bundle. (E) Higher magnification of the vascular bundles located at the center of the *jba-1D* stem (smaller box in C). The vascular bundles are radialized, with xylem cells (arrowheads) surrounding phloem cells. (G,H) Cross section through a radialized *jba-1D* leaf. Higher magnification of the vascular bundles (H) shows a polarity in the vascular bundle, with phloem cells at one side of the bundle and xylem cells protruding to the other side. Scale bars: 500  $\mu$ m (A,C); 50  $\mu$ m (B,D,E,H,F); 100  $\mu$ m (G).

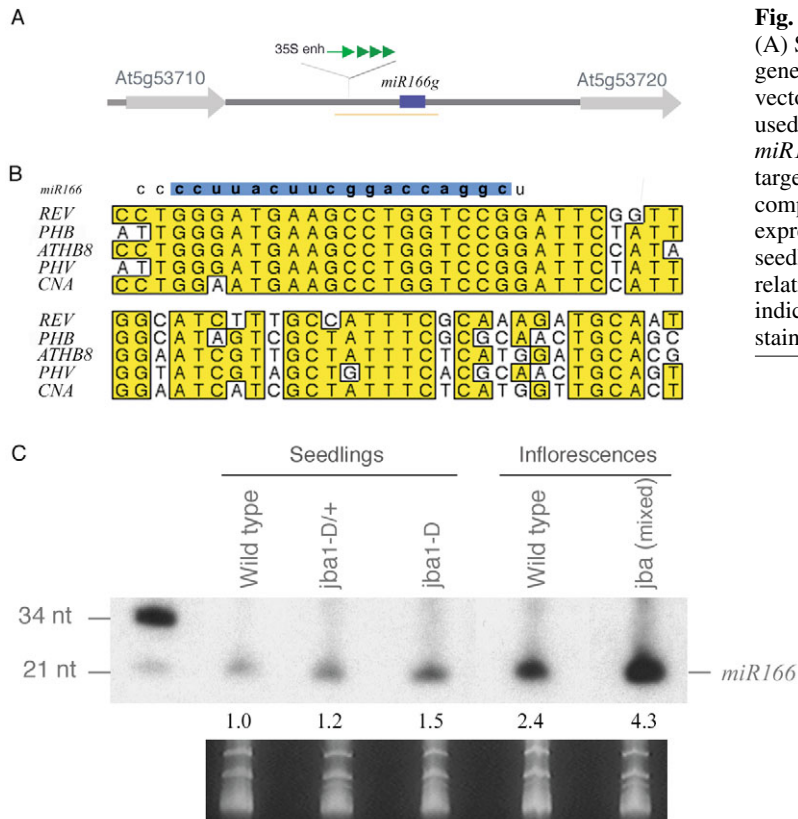


**Fig. 5.** Elevated expression of *miR166* in *jba-1D* plants. (A) Schematic of the insertion site of *jba-1D* relative to annotated genes. Green triangles indicate the 35S enhancers on the T-DNA vector. The orange line indicates the region of genomic DNA used to recapitulate the *jba-1D* phenotype. (B) Alignment of *miR166* with its putative *Arabidopsis* class III HD-ZIP gene target sequences. The blue box indicates the *miR166* sequence complementarity to the HD-ZIP genes sequences. (C) *miR166* expression. Blot of low molecular mass RNA extracted from seedlings and inflorescences of wild-type and *jba* plants. The relative amount of *miR166* accumulation in the various tissues is indicated below the autoradiograph. The ethidium bromide-stained gel is shown as loading control (bottom).

expression of *miR166g* might underlie the *jba* phenotypes. To test this hypothesis we transformed wild-type *Arabidopsis* plants with a genomic DNA fragment from *jba-1D* plants that began at the 35S enhancers and ended 129 bp downstream of the *MIR166g* sequences (Fig. 5A). The resulting T<sub>1</sub> and T<sub>2</sub> transformants were indistinguishable from *jba-1D/+* and *jba-1D* plants, demonstrating that over-expression of *miR166g* is sufficient to cause all of the *jba* phenotypes. We also performed a cross of *jba-1D/+* to plants carrying a hypomorphic allele of *DCL1*, which is required for miRNA biogenesis (Kurihara and Watanabe, 2004). Among the *jba-1D/+ dcl1-9/+* F<sub>1</sub> progeny of the cross, approximately 50% displayed a completely wild-type phenotype, while the other 50% had slightly enlarged stems but were otherwise normal (see Fig. S2 in supplementary material). This result confirms that miRNA processing is required to obtain the *jba* phenotypes, and in addition, it reveals that one copy of the *DCL1* enzyme is not enough to produce sufficient levels of *miR166g* to generate a phenotype.

The over-expression of *miR166* in *jba-1D* plants was confirmed by hybridizing a low-molecular mass RNA blot with a 21-nucleotide probe complementary to the mature *miR166* sequence (Fig. 5C). In *jba-1D* seedlings and inflorescence meristems, the level of the 21-nucleotide *miR166* was increased compared with wild type. In seedlings, measurement of the level of expression shows that *jba-1D* plants homozygous for the T-DNA insertion generated a higher level of *miR166* transcripts than hemizygous *jba-1D/+* plants, accounting for the dose dependence of the *jba* phenotypes. *miR166* is also expressed at much higher levels in both wild-type and *jba-1D* inflorescences than in seedlings (Fig. 5C).

**Embryo expression of *miR166* and an HD-ZIP target gene**

To investigate the role played by *miR166g* in regulating *Arabidopsis* morphogenesis, we determined the tissue distribution of the mature *miR166* sequence in wild-type and *jba-1D/+* plants using in situ hybridization. Because the *miR166g*-mediated *jba-1D* phenotype was detectable in mature embryos, we focused our analysis on the embryonic stage of development. The *miR166* expression pattern was identical in developing wild-type (Fig. 6A-E) and *jba-1D/+* (Fig. 6G-K) embryos, confirming that the 35S enhancer elements present in *jba-1D* up-regulate the affected gene in its normal expression

### Over-expression of *miR166g* causes the *jba-1D* phenotypes

The *jba-1D* T-DNA insertion falls in an intergenic region on chromosome 5 (Weigel et al., 2000). We determined that the T-DNA element was inserted 1890 base pairs (bp) downstream of At5g63710 and 1861 bp upstream of At5g63720 (Fig. 5A). Using RT-PCR we found that the At5g63720 gene is over-expressed in *jba-1D* mutant plants. However, transgenic *Arabidopsis* plants over-expressing At5g63720 under the control of the CaMV 35S promoter displayed a wild-type phenotype, indicating that this gene does not cause the *jba* phenotypes. Searching for other potential genes in the region we found a known microRNA locus, *MIR166g*, located 394 bp downstream of the T-DNA insertion site (Fig. 5A). *MIR166g* potentially targets members of the class III homeodomain-leucine zipper (HD-ZIP) family of transcription factors (Rhoades et al., 2002). Alignment of the mature *miR166g* RNA sequence with the members of the *Arabidopsis* class III HD-ZIP gene family shows 18 bp of complementarity with all five sequences (Fig. 5B). The miRNA complementarity site is found within the highly conserved putative sterol/lipid-binding START domain. Plants carrying dominant mutations in this region that reduce miRNA complementarity but do not change the amino acid sequence exhibit severe developmental phenotypes, suggesting that the gain-of-function phenotypes may be due to altered miRNA binding rather than altered protein function (Emery et al., 2003; Tang et al., 2003).

Mis-regulation of *REV*, *PHV* and *PHB* causes phenotypes in the same tissues in which we observed *jba-1D* phenotypes (Emery et al., 2003; McConnell and Barton, 1998; McConnell et al., 2001; Zhong and Ye, 2004), suggesting that over-



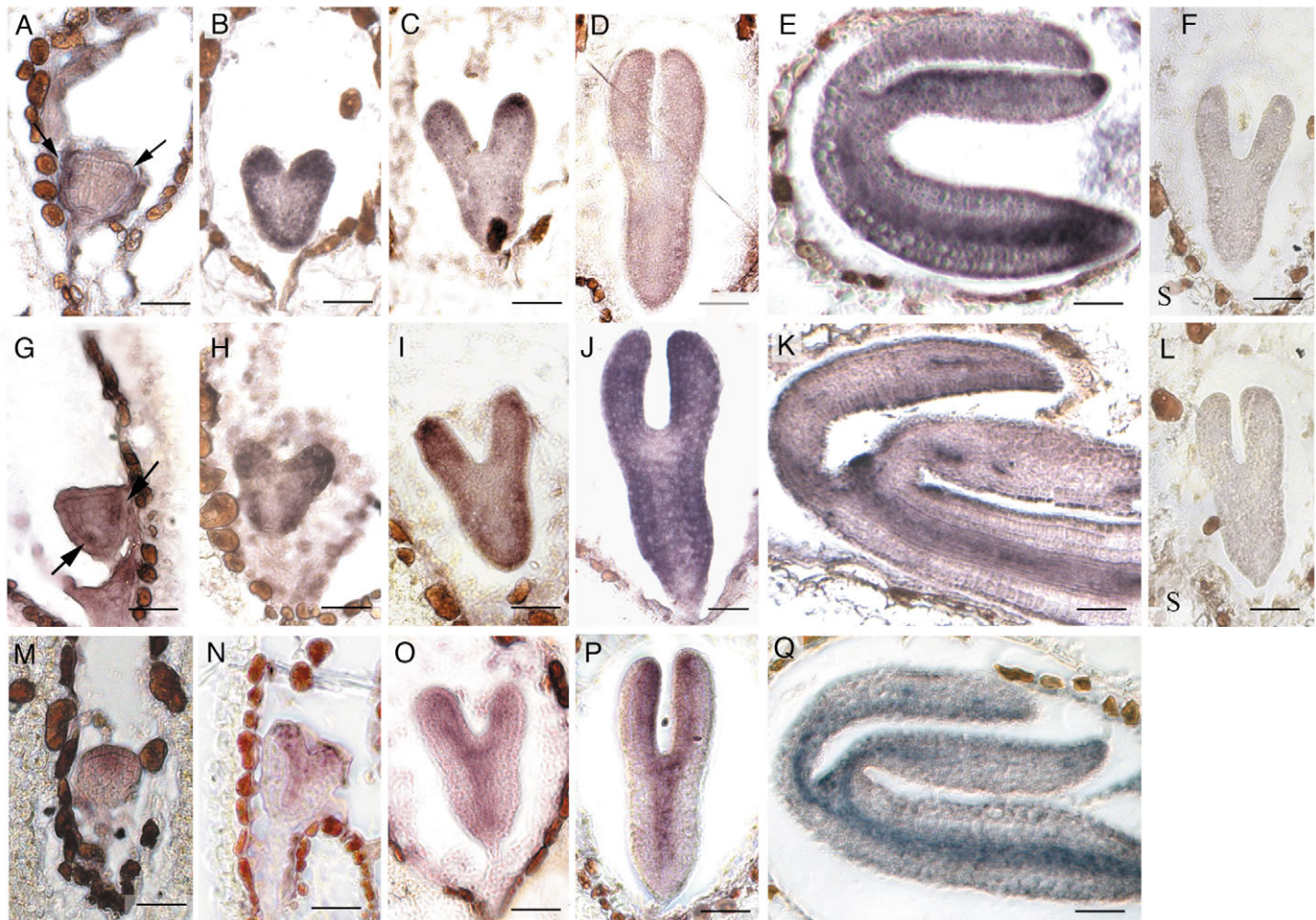


**Fig. 6.** Expression patterns of *miR166* and *REV* during embryogenesis. In situ localization of *miR166* in wild-type (A-E) and *jba-1D/+* (G-L) embryos. (A,G) At the late globular stage, *miR166* is expressed in the peripheral region of the hypocotyl and at the tips of the initiating cotyledons (arrows). (B-D,H-J) During the heart and torpedo stages, *miR166* expression expands to include the abaxial region and the distal tips of the cotyledons. (E,K) In mature embryos, *miR166* expression becomes localized to the SAM, the adaxial region of the cotyledons and the provascular tissues. (F,L) Control hybridization with a *miR166* sense probe, at the torpedo stage. (M-Q) *REV* expression in wild-type embryos. (M) *REV* is expressed in the central apical region of late globular stage embryos. (N) During the heart stage the *REV* expression expands to the adaxial region of the cotyledons and the central provascular tissues of the hypocotyl. (O,P) *REV* expression in early and late torpedo stages is similar to the heart stage. (Q) In mature embryos, *REV* is localized to the SAM, the adaxial regions of the cotyledons and the central provascular tissues. Scale bars: 500  $\mu$ m.

domain rather than inducing ectopic expression. The first stage at which we could reliably detect *miR166* transcripts was the late globular stage, where initial expression is restricted to the periphery of the hypocotyl and the tips of the initiating cotyledons (Fig. 6A,G). As the cotyledons emerge, expression expands to include the abaxial region and the distal tip (Fig. 6B,C,H,I). At the late torpedo stage, *miR166* was detected in the peripheral cells of the hypocotyl and along the adaxial and abaxial margins of the cotyledons (Fig. 6D,J). Weaker, if any, expression was detected in the central portion of the cotyledons corresponding to the developing vasculature. In mature embryos, the expression of *miR166* changed dramatically in both wild-type and *jba-1D/+* backgrounds. At this stage *miR166* accumulated in the SAM, the adaxial region of the cotyledons, and the provascular tissues of the embryos (Fig. 6E,K). These results demonstrate that *miR166* has a dynamic expression pattern during *Arabidopsis* embryogenesis.

The expression patterns of the *HD-Zip III* target genes in *Arabidopsis* embryos have been well characterized (Emery et al., 2003; McConnell et al., 2001; Prigge et al., 2005). To compare the distribution of *miR166* transcripts with those of its targets, we analyzed *REV* (Fig. 6M-Q) as its expression pattern encompasses all the others. During the late globular stage, *miR166* expression was restricted to the periphery of the hypocotyl and the tips of the initiating cotyledons, while *REV* was expressed in the apical, central region of the embryo (Fig. 6M). Thus the initial *REV* expression pattern is reciprocal to that of *miR166*. During the heart and torpedo stages, *REV* expression expanded to the adaxial region of the cotyledons, the presumptive SAM and the central provascular tissues of the hypocotyl (Fig. 6N,O,P). At these stages the *REV* domain is reciprocal to *miR166* in the hypocotyl and abaxial region of the cotyledons, but overlaps it in the adaxial region. These data suggest a possible role for *miR166* in clearing *REV* transcripts



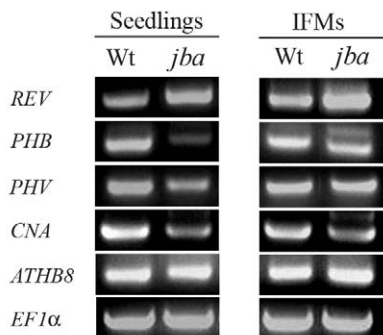


**Fig. 7.** Alteration of *miR166g* target gene expression levels in *jba-1D* plants. RT-PCR analysis of the class III HD-ZIP genes *REV*, *PHB*, *PHV*, *CNA* and *ATHB8* was performed on RNA extracts from whole seedlings and inflorescences (IFMs) of wild-type and *jba-1D* plants. *EF1α* was amplified as a control.

from the peripheral regions of the developing embryo. In mature embryos, *REV* was localized to the SAM, the adaxial regions of the cotyledons and the central provascular tissues (Fig. 6Q). At this stage the expression of *REV* was coincident with that of *miR166*, suggesting that the effect of *miR166* expression in mature embryos may be to modulate the mRNA transcript levels of *REV*.

We further investigated the effects of *miR166g* over-expression on the transcription levels of its target genes using semi-quantitative RT-PCR. The expression levels of *PHB*, *PHV* and *CNA* were significantly reduced in *jba-1D* seedlings compared to wild-type seedlings (Fig. 7). Decreased *PHB* and *CNA* transcript levels were also observed in *jba-1D* IFMs, while *PHV* transcript levels were slightly reduced. These results are consistent with the model that *miR166g* can direct cleavage and degradation of its target mRNAs. However, there were no differences in *ATHB8* transcript levels in *jba-1D* seedlings or IFMs, while *REV* transcript levels were elevated in *jba-1D* plants compared to wild-type plants (Fig. 7). Thus over-expression of *miR166g* leads to differential effects on the overall transcript levels of its *AtHD-ZIP* target genes.

Finally, to analyze whether the increase in *REV* transcript levels and the decrease in *CNA* and *PHB* transcript levels in *jba-1D* plants is due to alteration in their tissue distribution, we performed an in situ hybridization analysis on seedlings using *REV*, *CNA* and *PHB* probes. The *REV* expression pattern in wild-type (Fig. 8A) and *jba-1D* (Fig. 8B) seedlings was similar. In both backgrounds, the *REV* mRNA accumulated in the adaxial regions of the leaf primordia, in the vascular tissues and in the central zone of the SAM. These results show that the tissue distribution of *REV* mRNA is not altered in *jba-1D* seedlings. The *CNA* expression in wild-type seedlings was restricted to the adaxial region of developing leaves, to the vascular tissues and to the central, interior region of the SAM (Fig. 8C). In *jba-1D* seedlings, the *CNA* expression pattern changed significantly (Fig. 8D). *CNA* transcripts accumulated at a very low level in the adaxial region of initiating leaf primordia and in the adaxial region of developing leaves (data not shown), but no signal was detected in the vascular tissues or in the center of the SAM. The *PHB* expression pattern was also altered in *jba-1D* seedlings. Wild-type seedlings express *PHB* in the adaxial region of the leaf primordia, in the vascular

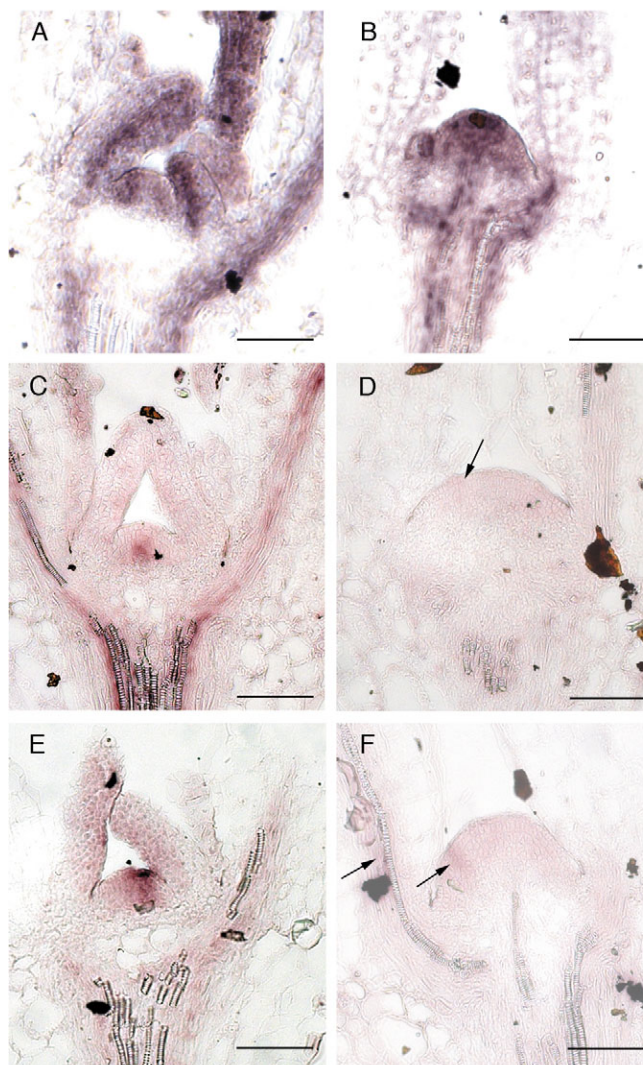


**Fig. 8.** *REV*, *CNA* and *PHB* expression patterns in wild-type and *jba-1D* seedlings. In situ localization of (A,B) *REV*, (C,D) *CNA*, and (E,F) *PHB* mRNA in longitudinal sections through 9-day-old seedlings. (A) Wild-type and (B) *jba-1D* seedlings showing *REV* expression in the central zone of the SAM, the adaxial regions of leaf primordia and the vascular tissues. (C) Wild-type seedling showing *CNA* expression in the central, interior cells of the SAM, the adaxial region of leaf primordia, and the vascular tissues. (D) In *jba-1D* seedlings, *CNA* is expressed at a low level in the adaxial region of initiating leaf primordia (arrow). *CNA* transcripts were not detected in the center of the SAM or in the vascular tissues. (E) Wild-type seedling showing *PHB* expression in the SAM, the adaxial region of leaf primordia, and the vascular tissues. (F) In *jba-1D* seedlings, *PHB* is expressed in the adaxial region of initiating leaf primordia (right arrow) and at a low level in the vascular tissues (left arrow). *PHB* transcripts were not detected in the SAM proper. For each probe, tissues from wild-type and *jba-1D* seedlings were analyzed on the same slide. Scale bars: 80  $\mu$ m.

tissues and in the SAM, mostly in the overlying layers (Fig. 8E). In *jba-1D* seedlings, *PHB* was expressed at only a very low level in the adaxial region of initiating leaf primordia on the flanks of the SAM and in the vascular tissues, but no transcripts are detected in the SAM itself. These results are

consistent with the RT-PCR data and demonstrate that over-expression of *miR166g* has differential effects on the transcript levels and tissue distributions of its *AtHD-ZIP* target genes.

## Discussion

A key role for miRNAs in plant development is inferred from the phenotypes of *dcl1* and *ago1* mutants, and from the over-expression or mutation of a number of miRNA loci. Here, we show that over-expression of *miR166g* in *jba-1D* mutants causes morphological defects in shoot apical meristems, stem vasculature, rosette leaves and gynoecia. Our experiments reveal a dynamic embryonic expression pattern of *miR166*, and a complex regulatory pathway controlling class III *HD-ZIP* gene transcription during development. They also identify an indirect role for *miR166g* in controlling *WUS* transcription and shoot meristem activity *via* regulation of class III *HD-ZIP* gene expression.

### Over-expression of *miR166g* causes severe developmental defects

Several independent lines of evidence demonstrate that the *jba-1D* phenotypes are caused by over-expression of *miR166g*. First, *miR166* transcripts are elevated in *jba-1D* seedlings and inflorescences, and this increase in transcript level occurs in a dose-dependent manner that corresponds with the increase in phenotype severity. Second, a 543 bp genomic region from the 35S enhancers through the *MIR166g* locus, but lacking coding sequences for any of the surrounding genes, is sufficient to recapitulate all aspects of the *jba* phenotype when introduced into wild-type Col plants. Third, DCL1 function is required to obtain the *jba* phenotypes, indicating that the effects of the *jba-1D* mutation require miRNA activity. Finally, mRNA expression levels of the targets of *miR166g*, the five members of the class III *HD-ZIP* family of transcription factors, are altered in *jba-1D* plants.

Over-expression of *miR166g* in *jba-1D* plants causes specific developmental defects. The earliest detectable phenotype is an increase in *jba-1D* mature embryo SAM size, indicating that the regulatory activity of *miR166* is already required during embryogenesis. The *jba-1D* SAM continues to enlarge throughout the vegetative and inflorescence phases, culminating in the splitting of the primary shoot apex into multiple independent SAMs and the fasciation of the inflorescence meristems. Meristem enlargement in *jba-1D* plants occurs through the coordinate expansion of *CLV3*-expressing cells in the overlying layers of the meristem and *WUS*-expressing cells in the interior, and requires wild-type *WUS* activity. The fasciated meristems of *clv* mutants also display coordinate expansion of *CLV3*-expressing and *WUS*-expressing cells, and are *WUS* dependent (Brand et al., 2000; Schoof et al., 2000). However, the fasciated meristems of *clv* plants and those of *jba-1D* plants are generated by different molecular mechanisms. The *CLV* pathway restricts the size of the *WUS*-expressing cell population by preventing its expansion laterally and upward into the L2 cell layer (Brand et al., 2000; Schoof et al., 2000). In contrast, *miR166* appears to regulate meristem size by indirectly controlling the amount of *WUS* transcription within the organizing center itself. Thus *miR166* and the *CLV* pathway function in parallel to regulate the level of *WUS* transcription and the number of *WUS*-

expressing cells in vegetative and inflorescence meristems, respectively.

The *jba-1D* mutation also causes the adaxialization of rosette leaves and vascular bundles in the stem, and a reduction in gynoecium tissue. Given that *PHB* and *PHV* confer adaxial identity (Emery et al., 2003; McConnell and Barton, 1998), the adaxialization of *jba-1D* leaves seems counterintuitive. However, experiments have shown that a SAM-derived signal(s) is important for specifying adaxial leaf identity (Snow and Snow, 1959; Sussex, 1954; Waites and Hudson, 1995), and thus initiating *jba-1D* leaves may receive an excess of adaxializing signal(s) emanating from multiple SAMs. Increased accumulation of transcripts from *REV*, which plays a redundant role with *PHB* and *PHV* in conferring adaxial fate (Emery et al., 2003), may also contribute to conditioning this phenotype, as increased meristem size per se is not sufficient to cause leaf adaxialization (Clark et al., 1993). Similarly, the decrease in *PHB*, *PHV* and *CNA* transcript levels observed in *jba-1D* plants is unlikely to be the sole cause of the reduced gynoecium phenotype, as *phb phv cna* mutants form extra carpels instead of fewer carpels (Prigge et al., 2005). *jba-1D* floral meristems are the same size as wild-type meristems, and thus the gynoecium defect is probably not due to premature floral meristem termination. *jba-1D* gynoecia consist of fewer cell types than normal and occasionally lack vasculature (data not shown), suggesting instead a possible defect in gynoecium patterning and/or polarity. Further work will be required to unravel the precise roles of *miR166* and the class III *HD-ZIP* genes in gynoecium development.

### *miR166* expression and regulation of the class III *HD-ZIP* genes

Our experiments show that over-expression of *miR166g* in activation-tagged *jba-1D* plants causes significant changes in the mRNA accumulation of their target class III *HD-ZIP* family members. We find that the overall transcription levels of the *HD-ZIP* genes are affected in *jba-1D* seedlings and inflorescences, but that the five target genes do not respond to *miR166g* over-expression in the same way. *ATHB8* transcript levels are unaffected by *miR166g* over-expression, suggesting that *ATHB8* may be targeted by other members of the *miR165/166* group, such as *miR166a* (Kim et al., 2005). *PHB*, *PHV* and *CNA* are all down-regulated in *jba-1D* seedlings and inflorescence meristems, while *REV* transcription is elevated. Since *REV* shows a similar expression pattern in wild-type and *jba-1D* seedlings (Fig. 8) and inflorescence meristems (data not shown), an explanation for the unexpected up-regulation of *REV* may be that *REV* is a target of negative regulation by *PHB*, *PHV* and/or *CNA*. This theory is consistent with previous observations that *CNA* and *ATHB8* partially suppress the *rev* and *rev phv* lateral and floral meristem defects, indicating an antagonistic relationship between them (Prigge et al., 2005).

Interestingly, we found that *miR166g* has a dynamic expression pattern in developing wild-type and *jba-1D* embryos. During the early stages of embryogenesis, *miR166* accumulates predominantly in the peripheral regions of the hypocotyls and throughout the developing cotyledons. The hypocotyl expression pattern of *miR166* is reciprocal to those of its five target genes, which are all expressed in overlapping patterns but are largely restricted to the central cells (Emery et al., 2003; Prigge et al., 2005). These data suggest that during



early embryogenesis *miR166* acts to clear the transcripts of its target gene(s) from the periphery of the developing hypocotyl. In contrast, the expression patterns of *miR166* and *REV*, *PHB*, *PHV* and *CNA* overlap in the developing cotyledons, indicating that the presence of the miRNA does not cause complete turnover of its target transcripts in these tissues. In mature embryos the *miR166* expression pattern alters dramatically, becoming confined to the SAM, the adaxial side of the cotyledons, and the vasculature. At this stage of development the expression pattern of *miR166* is coincident with that of its targets [*REV* in the SAM; *REV*, *PHB* and *PHV* in the cotyledons and all five genes in the vasculature (Prigge et al., 2005)] suggesting that a major effect of *miR166* expression at this stage may be to modulate the mRNA transcript levels of the class III *HD-ZIP* genes. The *Arabidopsis* class III *HD-ZIP* genes may thus represent examples of so-called miRNA 'tuning targets', messages for which miRNA regulation adjusts the protein output in a fashion that permits customized expression in different cells types yet a more uniform expression level within each cell type (Bartel and Chen, 2004). Alternatively, or additionally, the overlap of the miRNA and target mRNA expression patterns may suggest that the *HD-ZIP* genes are at this stage of development either targeted for translation repression or for methylation of their coding regions, as has been previously shown for the *PHB* and *PHV* loci (Bao et al., 2004).

### Regulation of shoot apical meristem activity by class III *HD-ZIP* genes

The most dramatic phenotype caused by over-expression of *miR166g* is the extensive SAM enlargement and stem fasciation. Previous work has implicated members of the class III *HD-ZIP* family in meristem regulation. *rev phb phv* mutants lack a functional embryonic SAM (Emery et al., 2003), indicating that *REV* plays a redundant role with *PHB* and *PHV* in SAM establishment. *rev* mutants have reduced lateral and floral meristem activity (Otsuga et al., 2001; Talbert et al., 1995), indicating that *REV* also promotes post-embryonic meristem initiation and function. *REV* gain-of-function mutations *avb1* and *rev-10D* lead to SAM enlargement, defective leaf polarity and altered vascular patterning (Emery et al., 2003; Zhong and Ye, 2004). These phenotypes resemble those observed in *jba-1D* plants, which accumulate higher than normal levels of *REV* transcripts. However, eliminating *REV* activity in a *jba-1D* background did not significantly attenuate the *jba* shoot meristem phenotypes. This result indicates that *REV* plays at most a minor role in conditioning the SAM enlargement and stem fasciation defects caused by over-expression of *miR166g*.

The shoot apical meristem phenotypes of *jba-1D* plants are also very similar to those of *phb phv cna* plants (Prigge et al., 2005). Like *jba-1D* mutants, *phb phv cna* mutants produce enlarged SAMs, fasciated meristems and internal vascular bundles in the stem. The redundant role of *PHB*, *PHV* and *CNA* in meristem regulation is independent of *REV* (Prigge et al., 2005), as is the role of *miR166g* (see Fig. S2 in supplementary material). Although *cna* mutations have no discernable effect on their own they enhance the stem cell accumulation defects of *clv* null mutant meristems, suggesting that *CNA* acts in parallel with the *CLV* pathway to regulate shoot apical meristem size (Green et al., 2005).

Our data confirm that proper regulation of class III *HD-ZIP* gene activity is a critical feature of normal shoot apical meristem function. We propose that in wild-type plants, *PHB*, *PHV* and *CNA* restrict SAM activity by down-regulating *WUS* transcription. During the late globular and heart stages of embryogenesis, *PHB*, *PHV* and *CNA* are all expressed in apical cells of the presumptive SAM (Prigge et al., 2005), in a pattern coincident with that of *WUS* (Mayer et al., 1998). After germination, *PHB* and *CNA* continue to be expressed in the meristem (Fig. 8) (McConnell et al., 2001), the *CNA* expression domain remaining coincident with that of *WUS*. Thus the transient expression of *PHB*, *PHV* and *CNA* early in embryogenesis, and the persistent expression of *PHB* and *CNA* in post-embryonic development, may be required to modulate the level of *WUS* transcription, leading to the maintenance of a stem cell population of the appropriate size. In *jba-1D* SAMs, over-expression of *miR166g* would cause a reduction in the level of *PHB*, *PHV* and *CNA* mRNAs and a resultant elevation of *WUS* transcription. Abnormally high levels of *WUS* activity could then promote excess stem cell accumulation and the eventual establishment of new stem cell foci, leading to SAM enlargement and ultimately to the splitting and fasciation of the *jba-1D* shoot apical meristem. We also find that this activity of *PHB*, *PHV* and *CNA* in regulating SAM size is largely independent of *REV*, consistent with data from analysis of *HD-ZIP* triple and quadruple mutant plants (Prigge et al., 2005).

Nine *MIR165/166* loci are present in the *Arabidopsis* genome, each of which has the potential to regulate any or all of its five class III *HD-ZIP* gene targets either by clearing the transcripts from specific cells or by regulating the level of transcript accumulation. To account for the observed expression of the *HD-ZIP* genes in combinatorial tissue- and stage-specific patterns, it seems reasonable to expect that the nine *MIR* loci will also have dynamic and differential transcription profiles. Further examination of the regulatory interactions between the various *MIR165/166* family members, their class III *HD-ZIP* target genes, and meristem maintenance factors will reveal additional insights into the complex interplay between polar lateral organs and the shoot apical meristem from which they derive.

We thank Marcey Sato and Hattie Brown for assistance with cloning and sectioning, Anita Fernandez, Kathy Barton and Michael Lenhard for supplying reporter lines, Xuemei Chen for protocols, and the ABRC for seed stocks. We are indebted to John Bowman for pointing out the location of *MIR166g* to us. This work was supported by Vaadia-BARD Postdoctoral Award No. FI-340-2003 from BARD, The United States–Israel Bi-national Agricultural Research and Development Fund to L.W. and by a USDA CRIS grant to J.C.F.

### Supplementary material

Supplementary material for this article is available at <http://dev.biologists.org/cgi/content/full/132/16/3667/DC1>

### References

- Achard, P., Herr, A., Baulcombe, D. C. and Harberd, N. P. (2004). Modulation of floral development by a gibberellin-regulated microRNA. *Development* **131**, 3357–3365.
- Aukerman, M. J. and Sakai, H. (2003). Regulation of flowering time and floral organ identity by a microRNA and its *APETALA2*-like target genes. *Plant Cell* **15**, 2730–2741.
- Baima, S., Nobili, F., Lucchetti, S., Ruberti, I. and Morelli, G. (1995). The

- expression of the *Athb-8* homeobox gene is restricted to provascular cells in *Arabidopsis thaliana*. *Development* **121**, 4171-4182.
- Baima, S., Possenti, M., Matteuchi, A., Wiseman, E., Altamura, M. M., Ruberti, I. and Morelli, G.** (2001). The *Arabidopsis* ATHB-8 HD-zip protein acts as a differentiation-promoting transcription factor of the vascular meristems. *Plant Physiol.* **126**, 643-655.
- Baker, C. C., Sieber, P., Wellmer, F. and Meyerowitz, E. M.** (2005). The *early extra petals1* mutant uncovers a role for microRNA *miR164c* in regulating petal number in *Arabidopsis*. *Curr. Biol.* **15**, 303-315.
- Bao, N., Lye, K.-W. and Barton, M. K.** (2004). MicroRNA binding sites in *Arabidopsis* class III HD-ZIP mRNAs are required for methylation of the template chromosome. *Dev. Cell* **7**, 653-662.
- Bartel, D. P.** (2004). MicroRNAs: Genomics, biogenesis, mechanism, and function. *Cell* **116**, 281-297.
- Bartel, D. P. and Chen, C. Z.** (2004). Micromanagers of gene expression: the potentially widespread influence of metazoan microRNAs. *Nat. Rev. Genet.* **5**, 396-400.
- Bohmert, K., Camus, I., Bellini, C., Bouchez, D., Caboche, M. and Benning, C.** (1998). *AGO1* defines a novel locus of *Arabidopsis* controlling leaf development. *EMBO J.* **17**, 170-180.
- Bowman, J. L., Smyth, D. R. and Meyerowitz, E. M.** (1989). Genes directing flower development in *Arabidopsis*. *Plant Cell* **1**, 37-52.
- Brand, U., Fletcher, J. C., Hobe, M., Meyerowitz, E. M. and Simon, R.** (2000). Dependence of stem cell fate in *Arabidopsis* on a feedback loop regulated by *CLV3* activity. *Science* **289**, 617-619.
- Carles, C. C. and Fletcher, J. C.** (2003). Shoot apical meristem maintenance: the art of a dynamic balance. *Trends Plant Sci.* **8**, 394-401.
- Cerutti, L., Mian, N. and Bateman, A.** (2000). Domains in gene silencing and cell differentiation proteins: The novel PAZ domain and redefinition of the Piwi domain. *Trends Biochem. Sci.* **25**, 481-482.
- Chen, X.** (2004). A microRNA as a translational repressor of APETALA2 in *Arabidopsis* flower development. *Science* **303**, 2022-2025.
- Clark, S. E., Running, M. P. and Meyerowitz, E. M.** (1993). *CLAVATA1*, a regulator of meristem and flower development in *Arabidopsis*. *Development* **119**, 397-418.
- Clough, S. J. and Bent, A. F.** (1998). Floral dip: a simplified method for *Agrobacterium*-mediated transformation of *Arabidopsis thaliana*. *Plant J.* **16**, 735-743.
- Emery, J. F., Floyd, S. K., Alvarez, J., Eshed, Y., Hawker, N. P., Izhaki, A., Baum, S. F. and Bowman, J. L.** (2003). Radial patterning of *Arabidopsis* shoots by class III HD-ZIP and KANADI genes. *Curr. Biol.* **13**, 1768-1774.
- Fletcher, J. C., Brand, U., Running, M. P., Simon, R. and Meyerowitz, E. M.** (1999). Signaling of cell fate decisions by *CLAVATA3* in *Arabidopsis* shoot meristems. *Science* **283**, 1911-1914.
- Green, K. A., Prigge, M. J., Katzman, R. B. and Clark, S. E.** (2005). CORONA, a member of the class III homeodomain-leucine zipper gene family in *Arabidopsis*, regulates stem cell specification and organogenesis. *Plant Cell* **17**, 691-704.
- Hammond, S. M., Bernstein, E., Beach, D. and Hannon, G. J.** (2000). An RNA-directed nuclease mediates post-transcriptional gene silencing in *Drosophila* cells. *Nature* **404**, 293-296.
- Han, M. H., Goud, S., Song, L. and Fedoroff, N.** (2004). The *Arabidopsis* double-stranded RNA-binding protein HYL1 plays a role in microRNA-mediated gene regulation. *Proc. Natl. Acad. Sci. USA* **101**, 1093-1098.
- Jackson, D.** (1992). In situ hybridization in plants. In *Molecular Plant Pathology: A Practical Approach* (ed. D. J. Bowles S. J. Gurr and R. McPherson), pp. 163-174. Oxford: Oxford University Press.
- Kim, J., Jung, J.-H., Reyes, J. L., Kim, Y.-S., Kim, S.-Y., Chung, K.-S., Kim, J. A., Lee, M., Lee, Y., Kim, V. N. et al.** (2005). microRNA cleavage of *ATHB15* mRNA regulates vascular development in *Arabidopsis* inflorescence stems. *Plant J.* **42**, 84-94.
- Kurihara, Y. and Watanabe, Y.** (2004). *Arabidopsis* micro-RNA biogenesis through Dicer-like 1 protein functions. *Proc. Natl. Acad. Sci. USA* **101**, 12753-12758.
- Mallory, A. C., Reinhart, B. J., Jones-Rhoades, M. W., Tang, G., Zamore, P. D., Barton, M. K. and Bartel, D. P.** (2004). MicroRNA control of *PHABULOSA* in leaf development: importance of pairing to the microRNA 5' region. *EMBO J.* **23**, 3356-3364.
- Martinez, J., Patkaniowska, A., Urlaub, H., Luhrmann, R. and Tuschl, T.** (2002). Single-stranded antisense siRNAs guide target RNA cleavage in RNAi. *Cell* **110**, 563-574.
- Mayer, K. F. X., Schoof, H., Haecker, A., Lenhard, M., Jurgens, G. and Laux, T.** (1998). Role of *WUSCHEL* in regulating stem cell fate in the *Arabidopsis* shoot meristem. *Cell* **95**, 805-815.
- McConnell, J. R. and Barton, M. K.** (1998). Leaf polarity and meristem formation in *Arabidopsis*. *Development* **125**, 2935-2942.
- McConnell, J. R., Emery, J., Eshed, Y., Bao, N., Bowman, J. L. and Barton, M. K.** (2001). Role of *PHABULOSA* and *PHAVOLUTA* in determining radial patterning in shoots. *Nature* **411**, 709-713.
- Otsuga, D., DeGuzman, B., Prigge, M. J., Drews, G. N. and Clark, S. E.** (2001). *REVOLUTA* regulates meristem initiation at lateral positions. *Plant J.* **25**, 223-236.
- Palatnik, J. F., Allen, E., Wu, X., Schommer, C., Schwab, R., Carrington, J. C. and Weigel, D.** (2003). Control of leaf morphogenesis by microRNAs. *Nature* **425**, 257-263.
- Park, W., Li, J., Song, R., Messing, J. and Chen, X.** (2002). CARPEL FACTORY, a Dicer homolog, and HEN1, a novel protein, act in microRNA metabolism in *Arabidopsis thaliana*. *Curr. Biol.* **12**, 1484-1495.
- Prigge, M. J., Otsuga, D., Alonso, J. M., Ecker, J. R., Drews, G. N. and Clark, S. E.** (2005). Class III homeodomain-leucine zipper gene family members have overlapping, antagonistic, and distinct roles in *Arabidopsis* development. *Plant Cell* **17**, 61-76.
- Reinhart, B. J., Weinstein, E. G., Rhoades, M. W., Bartel, B. and Bartel, D. P.** (2002). MicroRNAs in plants. *Genes Dev.* **16**, 1616-1626.
- Rhoades, M. W., Reinhart, B. J., Lim, L. P., Burge, C. B., Bartel, B. and Bartel, D. P.** (2002). Prediction of plant microRNA targets. *Cell* **110**, 513-520.
- Rojó, E., Sharma, V. K., Kovaleva, V., Raikhel, N. V. and Fletcher, J. C.** (2002). *CLV3* is localized to the extracellular space, where it activates the *Arabidopsis* CLAVATA stem cell signaling pathway. *Plant Cell* **14**, 969-977.
- Running, M. P., Clark, S. E. and Meyerowitz, E. M.** (1995). Confocal microscopy of the shoot apex. *Methods Cell Biol.* **49**, 217-229.
- Schauer, S. E., Jacobsen, S. E., Meinke, D. W. and Ray, A.** (2002). DICER-LIKE1: Blind men and elephants in *Arabidopsis* development. *Trends Plant Sci.* **11**, 487-491.
- Schoof, H., Lenhard, M., Haecker, A., Mayer, K. F. X., Jurgens, G. and Laux, T.** (2000). The stem cell population of *Arabidopsis* shoot meristems is maintained by a regulatory loop between the *CLAVATA* and *WUSCHEL* genes. *Cell* **100**, 635-644.
- Sessa, G., Steindler, C., Morelli, G. and Ruberti, I.** (1998). The *Arabidopsis* ATHB-8, -9 and -14 genes are members of a small gene family encoding highly related HD-Zip proteins. *Plant Mol. Biol.* **38**, 609-622.
- Sieburth, L. E. and Meyerowitz, E. M.** (1997). Molecular dissection of the AGAMOUS control region shows that *cis* elements for spatial regulation are located intragenically. *Plant Cell* **9**, 355-365.
- Smith, H. M. S. and Hake, S.** (2003). The interaction of two homeobox genes, *BREVIPEDICELLUS* and *PENNYWISE*, regulates internode patterning in the *Arabidopsis* inflorescence. *Plant Cell* **15**, 1717-1727.
- Snow, M. and Snow, R.** (1959). The dorsoventrality of leaf primordia. *New Phytol.* **58**, 188-207.
- Sussex, I. M.** (1954). Experiments on the cause of dorsiventrality in leaves. *Nature* **174**, 351-352.
- Talbert, P. B., Adler, H. T., Parks, D. W. and Comai, L.** (1995). The *REVOLUTA* gene is necessary for apical meristem development and for limiting cell divisions in the leaves and stems of *Arabidopsis thaliana*. *Development* **121**, 2723-2735.
- Tang, G., Reinhart, B. J., Bartel, D. P. and Zamore, P. D.** (2003). A biochemical framework for RNA silencing in plants. *Genes Dev.* **17**, 49-63.
- Turner, S. and Sieburth, L. E.** (2001). Vascular Patterning. In *The Arabidopsis Book* (ed. C. R. Somerville and E. M. Meyerowitz). Rockville, MD, USA: American Society of Plant Biologists.
- Vaucheret, H., Vazquez, F., Crete, P. and Bartel, D. P.** (2004). The action of *ARGONAUTE1* in the miRNA pathway and its regulation by the miRNA pathway are crucial for plant development. *Genes Dev.* **18**, 1187-1197.
- Vazquez, F., Gascioli, V., Crete, P. and Vaucheret, H.** (2004). The nuclear dsRNA binding protein HYL1 is required for microRNA accumulation and plant development, but not posttranscriptional transgene silencing. *Curr. Biol.* **14**, 346-351.
- Waites, R. and Hudson, A.** (1995). *phantastica*: a gene required for dorsoventrality of leaves in *Antirrhinum majus*. *Development* **121**, 2143-2154.
- Weigel, D., Ahn, J. H., Blazquez, M. A., Borevitz, J. O., Christensen, S. K., Fankhauser, C., Ferrandiz, C., Kardailsky, I., Malancharuvil, E. J., Neff, M. M. et al.** (2000). Activation tagging in *Arabidopsis*. *Plant Physiol.* **103**, 1003-1013.
- Zhong, R. and Ye, Z. H.** (2004). *amphivasal vascular bundle 1*, a gain-of-function mutation of the *IFL1/REV* gene, is associated with alterations in the polarity of leaves, stems and carpels. *Plant Cell Physiol.* **45**, 369-385.